### Title

Phosphorylation-dependent derepression by the response regulator HnoC in the Shewanella oneidensis nitric oxide signaling network




### Journal

Proceedings of the National Academy of Sciences of the United States of America, 110(48)

### ISSN

0027-8424



### Authors

Plate, Lars
Marletta, Michael A



### Publication Date

2013-11-26

### DOI

10.1073/pnas.1318128110

Peer reviewed

# Phosphorylation-dependent derepression by the response regulator HnoC in the *Shewanella oneidensis* nitric oxide signaling network

Lars Plate[a,b] and Michael A. Marletta[a,b,c,1]

[a]Department of Chemistry, The Scripps Research Institute, La Jolla, CA 92037; and Departments of [b]Molecular and Cell Biology and [c]Chemistry, University of California, Berkeley, CA 94720

Contributed by Michael A. Marletta, September 27, 2013 (sent for review August 10, 2013)

**Nitric oxide (NO) is an important signaling molecule that regulates diverse physiological processes in all domains of life. In many gammaproteobacteria, NO controls behavioral responses through a complex signaling network involving heme-nitric oxide/oxygen binding (H-NOX) domains as selective NO sensors. In *Shewanella oneidensis*, H-NOX–mediated NO sensing increases biofilm formation, which is thought to serve as a protective mechanism against NO cytotoxicity. The H-NOX/NO-responsive (*hno*) signaling network involves H-NOX–dependent control of HnoK autophosphorylation and phosphotransfer from HnoK to three response regulators. Two of these response regulators, HnoB and HnoD, regulate cyclic-di-GMP levels and influence biofilm formation. However, the role of the third response regulator in the signaling network, HnoC, has not been determined. Here we describe a role for HnoC as a transcriptional repressor for the signaling genes in the *hno* network. The genes controlled by HnoC were identified by microarray analysis, and its function as a repressor was confirmed in vivo. HnoC belongs to an uncharacterized family of DNA-binding response regulators. Binding of HnoC to its promoter targets was characterized in vitro, revealing an unprecedented regulation mechanism, which further extends the functional capabilities of DNA-binding response regulators. In the unphosphorylated state HnoC forms a tetramer, which tightly binds to an inverted-repeat target sequence overlapping with the promoter regions. Phosphorylation of HnoC induces dissociation of the response regulator tetramer and detachment of subunits from the promoter DNA, which subsequently leads to transcriptional derepression.**

transcription factor | feedback | two-component signaling | MerR

Many microbes switch from a motile to a sessile lifestyle. In that process, large numbers of cells form surface-adhered clusters known as biofilms. Microbes in biofilms are protected from hostile environmental factors (e.g., antibiotic treatment) owing to encapsulation in an extracellular polysaccharide matrix and prevalent metabolic dormancy (1). As such, biofilms are associated with chronic infections of pathogens (2), and many therapeutic strategies for fighting infectious diseases are now focused on treating the bacterial biofilm state (3).

The switch from a motile lifestyle to surface attachment and biofilm formation can be influenced by many factors, including nutrient availability, quorum sensing, or specific signaling molecules (4). Signaling cues often affect the concentration of the bacterial secondary messenger cyclic-di-GMP, which stimulates biofilm formation. One molecule that has been implicated in controlling biofilm formation is nitric oxide (NO). In very low concentrations, this reactive gas molecule is an important signaling agent in both prokaryotes and eukaryotes. In contrast, high concentrations of NO are cytotoxic, a property exploited by macrophages in response to microbial infections (5). Therefore, NO forms a link between the innate immune response and biofilms as a possible microbial defense mechanism (6).

NO has been shown to both promote and inhibit biofilm formation. In *Pseudomonas aeruginosa*, NO has been associated with biofilm dispersal by decreasing cyclic-di-GMP levels, although the nature of the NO sensor and the signaling mechanism are unknown (7). In *Legionella pneumophila* and *Shewanella woodyi*, heme-nitric oxide/oxygen binding (H-NOX) proteins have been identified as selective NO sensors. The H-NOX protein controls the activity of a diguanylate cyclase and phosphodiesterase, thus influencing cyclic-di-GMP levels and biofilm dispersal (8, 9). In contrast, NO stimulates biofilm formation in *Shewanella oneidensis* and *Vibrio cholerae* (6). Here, H-NOX proteins act as sensors in a more sophisticated multicomponent signaling system that elevates cyclic-di-GMP levels in response to NO. The mechanistic details of the H-NOX/NO (*hno*) signaling system have been recently characterized (6) (Fig. 1*A*). The H-NOX protein (HnoX) controls the activity of the histidine kinase HnoK in a ligand-dependent manner (10). NO-bound HnoX inhibits HnoK phosphorylation, whereas the unliganded HnoX allows HnoK to become phosphorylated. Subsequently, HnoK transfers its phosphoryl group to three response regulator targets: HnoB, HnoC, and HnoD. A second histidine kinase, HnoS, which has an unidentified signal input, also phosphorylates the three response regulators.

Response regulators mediate the functional output of the bacterial signaling system through effector domains (11, 12), which often harbor enzymatic activity, as is the case for HnoB. Phosphorylation of HnoB activates a phosphodiesterase domain, leading to increased cyclic-di-GMP hydrolysis. The second response regulator in the *hno* network, HnoD, functions as phos-

## Significance

**The majority of response regulators in bacterial two-component signaling systems function as transcription factors to induce changes in gene expression in response to an external stimulus. Phosphorylation typically promotes subunit oligomerization, which enhances DNA binding. Here we describe a response regulator, HnoC, with an unprecedented regulation mechanism. Unphosphorylated HnoC exists as a tetramer and associates tightly to DNA, whereas phosphorylation causes subunit dissociation and transcriptional derepression. HnoC is part of a multicomponent signaling network, which controls biofilm formation in response to nitric oxide, possibly as a defense mechanism against NO cytotoxicity. HnoC represses transcription of all of the genes in the NO-signaling network, thus creating a transcriptional feedback loop, which could further tune the signaling dynamics.**

Author contributions: L.P. and M.A.M. designed research; L.P. performed research; L.P. and M.A.M. analyzed data; and L.P. and M.A.M. wrote the paper.

The authors declare no conflict of interest.

Data deposition: Microarray data from this study have been deposited in the Gene Expression Omnibus (GEO) database, www.ncbi.nlm.nih.gov/geo (accession no. GSE44689).

[1]To whom correspondence should be addressed. E-mail: marletta@scripps.edu.

This article contains supporting information online at www.pnas.org/lookup/suppl/doi:10.1073/pnas.1318128110/-/DCSupplemental.

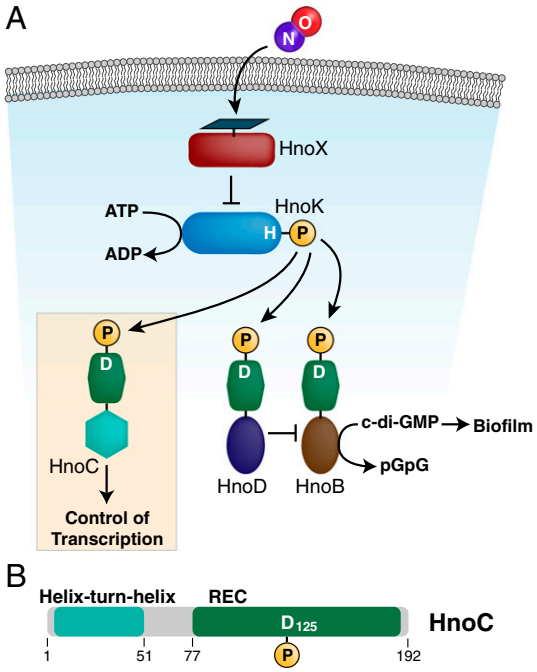


**Fig. 1.** The role of HnoC as a transcriptional regulator in the H-NOX/NO signaling network. (*A*) Summary of the H-NOX/NO signaling network controlling biofilm formation. The histidine kinase HnoK phosphorylates three response regulators: HnoB, HnoC, and HnoD. Phosphorylation activates the phosphodiesterase activity of HnoB and circumvents the inhibition of HnoB by HnoD. The stimulated HnoB activity leads to increased hydrolysis of cyclic-di-GMP and low biofilm levels. NO binding to HnoX inhibits the autophosphorylation of HnoK, lowers the phosphodiesterase activity of HnoB, and increases biofilm formation. HnoC constitutes a separate arm in the signaling network, controlling a transcriptional response. (*B*) The domain organization of HnoC (SO_2540). In addition to the C-terminal phosphoreceiver domain (REC) containing the site of phosphorylation (D125), HnoC contains an N-terminal HTH DNA binding domain.

phorylation-dependent allosteric effector of HnoB to fine-tune cyclic-di-GMP hydrolysis. NO stimulus decreases HnoK kinase activity, lowering the phosphorylation levels of HnoB and HnoD. The diminished activity of HnoB and HnoD causes a rise in cyclic-di-GMP levels, ultimately leading to cellular attachment in biofilms (6) (Fig. 1*A*).

In a number of gammaproteobacteria, such as *S. oneidensis*, a third response regulator, HnoC (SO_2540), adds further complexity to the *hno* signaling network. HnoC contains a DNA-binding effector domain, indicating that it could serve as a transcriptional regulator (13). DNA-binding response regulators can be further classified into subfamilies on the basis of structural classification of their DNA-binding domains. The most prevalent families contain variations of helix-turn-helix (HTH) motives, such as winged-HTH in the OmpR/PhoB family, simple HTH in the NarL/FixJ family, and the two domain AAA-FIS effector in the NtrC family (13). HnoC belongs to a relatively small subfamily of DNA-binding response regulators possessing an HTH domain from the MerR family (Pfam: HTH_17) (13, 14). Currently there are 70 members of this family listed in the Pfam database.

HnoC is predicted to function as a transcriptional regulator in the *hno* signaling network. However, the gene regulation targets of HnoC, as well as its functional role on NO-induced biofilm formation, are unknown. This study establishes the transcriptional targets of HnoC and demonstrates that HnoC represses expression of all components of the *hno* network, thus forming a transcriptional feedback loop. Furthermore, the molecular mechanism for HnoC transcriptional repression was investigated, revealing several unprecedented regulation features in this previously uncharacterized MerR subfamily of response regulators.

## Results

**Identification of Transcriptional Targets of HnoC.** The HnoC response regulator consists of a C-terminal phosphoreceiver domain and an N-terminal helix-turn-helix domain (Pfam HTH_17) from the MerR superfamily (Fig. 1*B*) (13, 14). The presence of this DNA-binding effector domain in the response regulator strongly indicates that HnoC acts as a transcriptional regulator. To identify the target genes controlled by HnoC, mRNA transcript levels in *S. oneidensis* were measured using whole-genome microarray analysis. Gene expression levels of a WT strain were compared with an *hnoC* deletion strain. Both strains were grown anaerobically to exponential phase, and total RNA was stabilized and harvested. RNA probes were generated and hybridized to a custom microarray covering the complete *S. oneidensis* genome. Four biological replicates from each strain were compared, and differentially expressed transcripts were identified using a false-discovery rate of 0.05 (Fig. 2*A* and Dataset S1). Deletion of *hnoC* led to up-regulation of only seven genes, indicating that HnoC functions as a highly specific transcriptional regulator for a small set of genes. Intriguingly, six of the seven up-regulated features in the *hnoC* knockout strain are contained within the three *hno* operons (Fig. 2*B*). Moreover, four of the protein products have confirmed roles in the H-NOX/NO (*hno*) signaling network, namely the NO-sensor HnoX, the kinase HnoS, and the response regulators HnoB and HnoD (6). SO1695 is the only up-regulated gene target outside the *hno* operons. Subsequent characterization failed to confirm any regulation of SO1695 by HnoC, suggesting a false-positive dysregulation in the microarray data. The up-regulation of genes in the *hno* operons implies that HnoC acts as a transcriptional repressor for all genes in the H-NOX/NO signaling network. The other genes in the hno operons (*hnoK*, *hnoT*) could also be dysregulated in the *hnoC* knockout strain, but their changed expression levels fall just outside the specified cufoff (Dataset S1). Because *hnoC* is itself cotranscribed from the

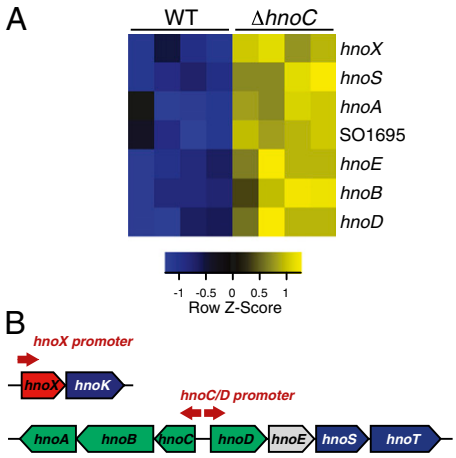


**Fig. 2.** Gene expression profiling results of *hnoC S. oneidensis* knockout. (*A*) Heat-map summarizing the genes that show differential expression between a WT *S. oneidensis* strain and an *hnoC* knockout strain (Δ*hnoC*). Total RNA was isolated from the respective strains, labeled, and hybridized to a whole-genome microarray of *S. oneidensis*. Differentially expressed transcripts were filtered using a fold-change >2 and adjusted $P < 0.05$. Expression levels in each row were normalized to their Z-score (yellow, high expression; blue, low expression). Four biological replicates for each strain are grouped in the columns. (*B*) The *hno* genes are organized into three separate operons containing two distinct promoter regions: the isolated *hnoX* promoter and the bidirectional *hnoC/hnoD* promoters.

*hno* operons, HnoC thus creates an autoregulatory transcriptional feedback loop.

**HnoC Acts as Transcriptional Repressor in Vivo.** The *hno* genes of the signaling network are organized in three operons that lie in two separate loci on the *S. oneidensis* chromosome (Fig. 2*B*). HnoX and HnoK are cotranscribed from an isolated operon under control of the *hnoX* promoter, henceforth termed *hnoXp*. The other two operons share a bidirectional promoter region containing the *hnoC* and *hnoD* promoters (*hnoCp* and *hnoDp*). To test whether HnoC directly regulates each of the three *hno* promoters in *S. oneidensis*, we examined GFP expression driven by each *hno* promoter in a reporter assay. Stretches of 250 bp containing either the *hnoXp*, *hnoCp*, or *hnoDp* region were cloned separately into a plasmid to control eGFP expression (15). The reporter plasmids were transformed into WT *S. oneidensis*, as well as into *hnoX*, *hnoK*, and *hnoC* in-frame deletion strains. The reporter strains were grown aerobically until exponential phase, and GFP expression was assessed by flow cytometry.

GFP expression was undetectable in the absence of a promoter in the reporter plasmid or when a random *hnoD* intragenic sequence was inserted as a negative control (Fig. 3*A*). In contrast, addition of *hnoXp*, *hnoCp*, and *hnoDp* led to measurable GFP expression, albeit of varying intensities, suggesting that the relative strengths of the promoters differ. In the WT strain, *hnoCp* produced the highest fluorescent intensities, whereas expression from *hnoXp* and *hnoDp* was 20 times and 9 times lower, respectively. In the *hnoC* knockout, GFP expression was significantly elevated compared with WT *S. oneidensis* in the case of all three promoters (1.5-, 6.8-, and 7.1-fold for *hnoXp*, *hnoCp*, and *hnoDp*, respectively). The observed increase in transcription in the absence of HnoC confirms its role as a transcriptional repressor in vivo. Deletion of HnoK did not influence GFP expression, even though HnoK functions as an upstream kinase of HnoC. However, a second kinase, HnoS, that can also phosphorylate HnoC is still present in this strain and might mask any effects on GFP expression (6). In contrast, a measurable increase in fluorescence was observed from the *hnoC* promoter when HnoX was deleted. This suggests a role for HnoX as an upstream inhibitor of HnoC. This effect is consistent with the signaling network, in which HnoX inhibits HnoK, which in turn phosphorylates HnoC. A similar increase might be concealed for the *hnoX* and *hnoD* promoter owing to their lower overall induction of GFP expression.

GFP is a very stable protein with a half-life greater than 24 h (16). Consequently, the relatively small increase in GFP expression in the HnoC knockout might be masked by high background GFP levels in the WT strain due to continual accumulation during growth. To test the true repressive power of HnoC, expression of an unstable GFP(AAV) variant that possesses a much shorter half-life (~190 min) was measured (16). The expression was driven by *hnoCp* (Fig. 3*B*). In this case, no measurable fluorescence could be detected in the WT, the *hnoX* deletion strain, or the *hnoK* deletion strain, which confirms that much of the previously observed signal was due to slow degradation of accumulated GFP. On the other hand, the *hnoC* knockout produced very high fluorescence levels, comparable to levels of the stable GFP variant and to constitutive GFP expression from a transposon insertion. Overall, deletion of HnoC caused a 440-fold increase in GFP expression, corresponding to a high dynamic range between active transcription and full repression by HnoC.

The activation of GFP expression in the *hnoC* deletion strain could be reversed by complementation with a plasmid-derived copy of the *hnoC* gene (Fig. 3*C*). WT HnoC lowered expression to similar levels as in WT *S. oneidensis*. Complementation with D125A HnoC, which lacks the phosphorylation site, represses GFP expression to similar levels. This observation suggests that WT HnoC is mostly present in the unphosphorylated state under

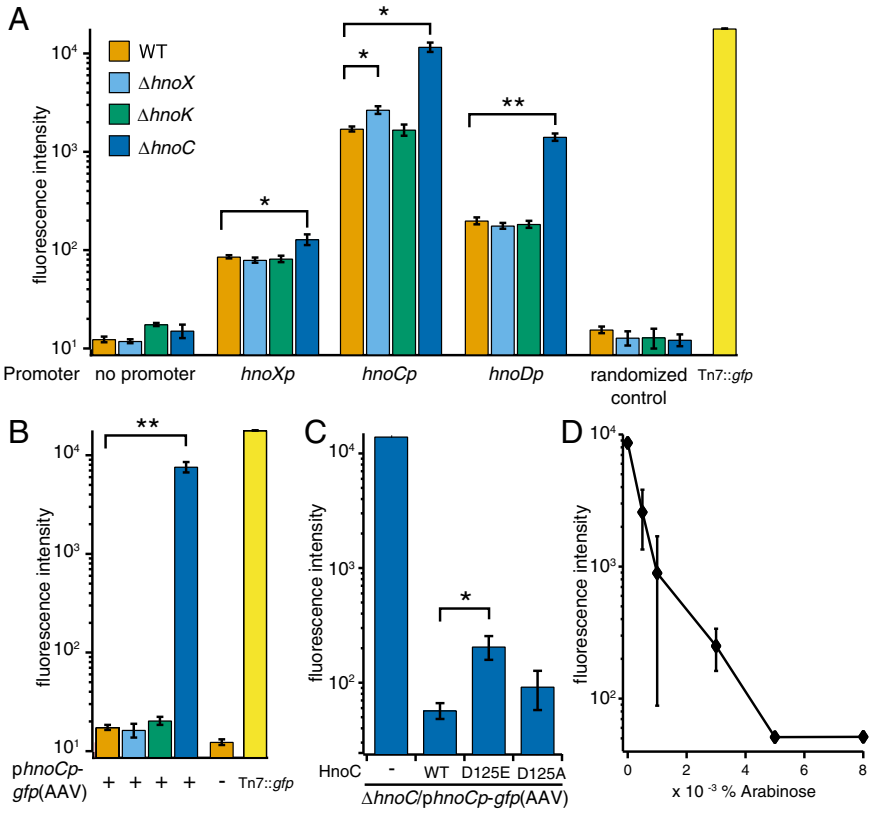


**Fig. 3.** Reporter assay measuring GFP expression from the HnoC-regulated promoters in *S. oneidensis* strains. Reporter plasmids were constructed by cloning the *hnoX*, *hnoC*, *hnoD* promoter or a negative control promoter into pProbeNT to drive eGFP expression (*A*) or the expression of an unstable GFP (AAV) variant (*B*). The plasmids were transformed into WT, Δ*hnoX*, Δ*hnoK*, or Δ*hnoC S. oneidensis* strains, and GFP expression was quantified by flow cytometry. Median fluorescence intensities were normalized to a *S. oneidensis* strain that expressed GFP constitutively (Tn7::*gfp*). (*C*) Complementation of the Δ*hnoC S. oneidensis* strain with WT HnoC, phosphorylation-inactive D125A, or the phosphorylation-mimic D125E HnoC. The pProbe-NT::*hnoCp-gfp (AAV)* construct served as reporter, and HnoC expression was induced from pBAD33. (*D*) Flow cytometry of *E. coli* DH10B cotransformed with pProbe-NT:: *hnoCp-gfp(AAV)* and pBAD33-HnoC. HnoC expression was induced in individual cultures with arabinose concentrations ranging from 0.0005% to 0.008% (wt/vol). Intensities from three biological replicates were averaged, and the SE is represented as error bars. Results from a two-tailed unpaired *t* test to compare the intensities between strains are shown by asterisks (*$P < 0.05$, **$P < 0.005$).

the reporter assay conditions and could further explain why the *hnoK* knockout does not lead to a measurable decrease in GFP expression. In contrast, the aspartate to glutamate mutant of the phosphorylation site (D125E), which can mimic the phosphorylated state of response regulators (6, 17, 18), only partially lowers GFP expression. This weaker repression serves as an indication that the phosphorylated state of HnoC derepresses transcription.

To test whether HnoC repression is concentration-dependent, the *hnoCp-gfp* reporter plasmid and a plasmid for arabinose-inducible expression of HnoC were cotransformed into *Escherichia coli* DH10B. Cultures were grown to exponential phase, and HnoC was induced with varying arabinose concentrations. In the absence of arabinose and HnoC, GFP expression was high (Fig. 3*D*). This demonstrated that *hnoCp* was also active in *E. coli*. Overexpression of HnoC led to a decrease in the fluorescence intensities and lower GFP expression. The extent of the decrease was dependent on the amount of inducer for HnoC expression. Overall, the reporter assays confirmed that HnoC functions as a strong repressor of the three *hno* promoters in vivo, and the degree of repression can be tuned by altering its concentration.

**HnoC Binding to *hno* Promoter Regions.** The molecular mechanism by which HnoC represses transcription from the *hno* promoters was then investigated. Response regulators with DNA-binding domains typically associate directly to the promoter region or to a control region in close proximity. Activators such as members of the OmpR/PhoB or NtrC family initiate transcription by recruiting RNA polymerase (RNAP) (19, 20) or by stimulating open complex formation of an RNAP-promoter complex (21). In contrast, a repressor such as CovR prevents RNA polymerase from recognizing the promoter (22).

To test whether HnoC directly interacted with the *hno* promoter DNA, gel-shift assays were conducted between HnoC and *hno* promoter probes. Fluorescently labeled 250- to 300-bp probes of the control regions around each promoter were generated. The *hnoXp* probe stretches from the −200 to the +50 position of the *hnoX* gene. The *hnocC/Dp* probe contains the intergenic region between *hnoC* and *hnoD* extending from the +50 position in each gene. HnoC (50 nM) was incubated with each control region, and the mixture was separated by native polyacrylamide electrophoresis (Fig. 4*A*). HnoC produced a clear gel-shift with both the *hnoXp* and *hnoC/Dp* probe, revealing a direct interaction between the protein and DNA. For both control regions, the labeled probe binding was competed when 25-fold excess of unlabeled probe was added. In contrast, addition of nonspecific DNA had no effect on the HnoC–DNA interaction, confirming that the interaction is specific.

To determine the dissociation constants between HnoC and the control region probes, HnoC amounts were titrated to the *hnoXp* and *hnoC/Dp* probes in the gel-shift experiment, and binding curves between HnoC and the *hnoXp* probe (Fig. 4*B*) and the *hnoC/Dp* probe (Fig. 4*C*) were generated. The curves clearly show the sigmoidal shape typical for cooperative binding interactions. The data were fit to a cooperative binding model to determine dissociation constants of 2.5 and 8.8 nM and Hill coefficients of 3.2 and 2.8 for the *hnoX* and *hnoC/D* control regions, respectively (Fig. 4 *B* and *C* and Table 1). The cooperative binding behavior and magnitude of the Hill coefficient suggest that HnoC multimerizes and that at least three to four subunits participate in the association to the control region DNA.

**Identification of HnoC Binding Sites by DNA Footprinting.** To determine the exact binding sites of HnoC in the control region around the *hnoX* and *hnoC/D* promoters, DNA footprinting was carried out. Probes of the respective promoter control regions were digested with DNase I in the presence of increasing amounts of HnoC to reveal which areas were protected by binding of the transcription factor. In both control regions, addition of HnoC produced a protected area corresponding to ~27 nucleotides

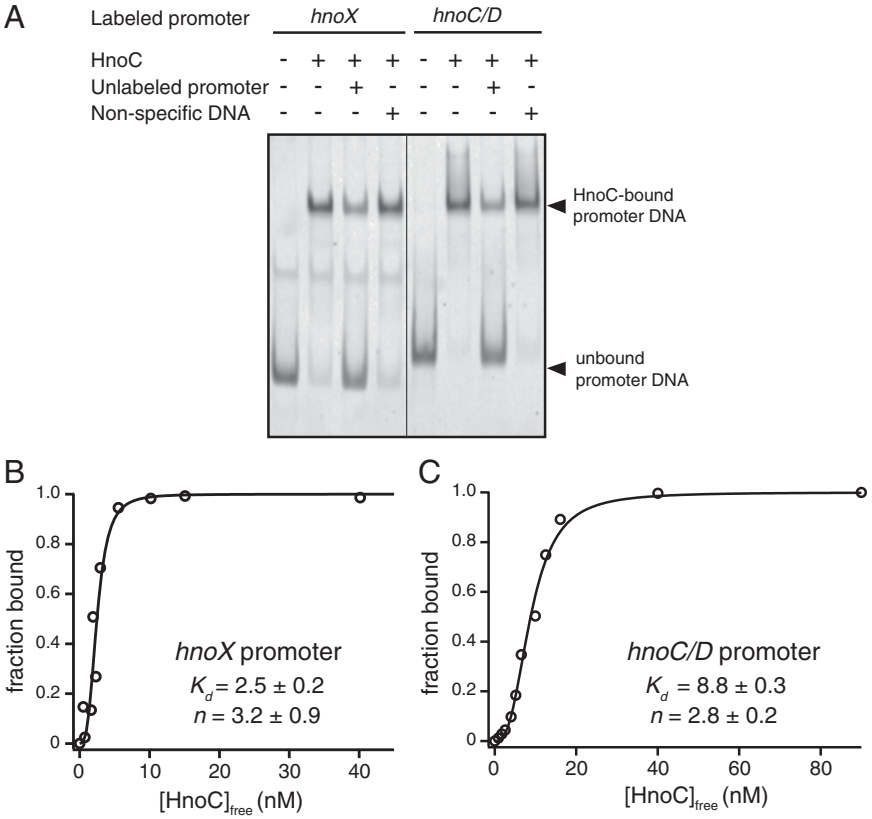


**Fig. 4.** Gel-shift binding assays between HnoC and promoter region DNA probes. Fluorescently labeled DNA probes (5 nM) were incubated with HnoC (50 nM) and separated by native PAGE. (*A*) A gel-shift occurred between HnoC and the *hnoX* control region, as well as the *hnoC/D* control region probe. This gel-shift was reduced with 25-fold excess unlabeled probe. (*B* and *C*) Binding curves between HnoC and the *hnoX* (*B*) or the *hnoC/D* control region (*C*). Bound and unbound DNA amounts were quantified by densitometry and fit to a cooperative binding model.

**Table 1. Dissociation constants of HnoC from control DNA**

| | Unphosphorylated | | Phosphorylated* | |
|---|---|---|---|---|
| Promoter | $K_D$ (nM) | Hill coefficient | $K_D$ (nM) | Hill coefficient |
| *hnoXp* | 2.5 ± 0.2 | 3.2 ± 0.9 | 11.5 ± 1.5 | 2.2 ± 0.4 |
| *hnoC/Dp* | 8.8 ± 0.3 | 2.8 ± 0.2 | 10.4 ± 0.4 | 3.0 ± 0.4 |

*Binding curves for the phosphorylated state of HnoC were generated by summing up the intensities of the three DNA bound species. Dissociation constants were calculated from a fit to a cooperative binding model.

(Fig. 5 *A* and *B*). The protected region in the *hnoX* promoter is located 5 nucleotides downstream of the −10 site and overlaps with the transcription start site. The binding location in the *hnoC/D* control region overlaps with the −10 site of the *hnoD* promoter and the −35 site of the *hnoC* promoter (Fig. 5 *C* and *D*). Consequently, HnoC binding could interfere with association of the RNAP holoenzyme and transcription initiation.

Transcription factor dimers often bind to tandem repeat sequences. For example, OmpR/PhoB family members bind to direct repeats, where each HTH domain recognizes a 7- to 10-bp consensus sequence (19, 23, 24). On the other hand, MerR dimers and NarL response regulator dimers bind to inverted repeats (25, 26). Alignment of the protected DNA regions by HnoC in the *hnoX* and *hnoC/D* promoters shows several conserved stretches (Fig. 5*E*). Intriguingly, a 20-bp area consists of two inverted repeats. This suggests that two HnoC subunit interact with the promoter DNA in a head-to-head orientation similar to other MerR family members (27).

The *S. oneidensis* genome was searched for other occurrences of this HnoC binding consensus sequence. The only other highly confident incidence of this motif was identified in the promoter region of SO_2547, an operon directly adjacent to the *hnoDEST* operon. A gel-shift assay confirmed HnoC binding to this promoter region (Fig. S1), suggesting that HnoC also controls expression of this operon, which encodes three chemotaxis genes. On the basis of the three binding sites of HnoC, each consisting of an inverted repeat, a consensus sequence for the half-site recognized by an HnoC momoner could be generated (Fig. 5*F*). This analysis highlights that adenosine residues at position 1 and 10, as well as a G[TA]C motif in the center, are required for HnoC binding.

**Effect of Phosphorylation on HnoC DNA Binding.** HnoC is the phosphorylation target of two histidine kinases in the *hno* signaling network, HnoK and HnoS (6). To assess the regulatory consequences of phosphorylation, the previous DNA-binding experiment was repeated with the phosphorylated form of HnoC. For this purpose, HnoC was preincubated with a large excess of HnoK and ATP before addition of the *hno* promoter DNA probes. Phosphotransfer assays using [$\gamma$-$^{32}$P]-ATP demonstrated that excess HnoK could stably phosphorylate HnoC (Fig. S2*A*). The extent of HnoC phosphorylation under these conditions exceeded 80% after 30 min, validating that HnoC was mostly present in the phosphorylated state (Fig. S2*B*).

Unphosphorylated HnoC formed a homogeneous DNA-control region complex with both *hnoXp* and *hnoC/Dp*, indicated by the presence of a single band at high retention in the native gel when increasing concentrations of HnoC were added to the probe (Fig. 6 *A* and *B*, *Left*). In contrast, when HnoK and ATP were added to phosphorylate HnoC, two additional DNA-bound species with lower retention were separated in the gel (Fig. 6 *A* and *B*, *Right*). Addition of an inactive histidine kinase mutant (H72A HnoK) did not lead to the formation of any additional DNA-bound species, confirming the dependence on phosphorylation. The presence of these species can be attributed to a different HnoC:DNA binding stoichiometry or to alternate conformations of the phosphorylated HnoC–DNA complex. Furthermore, the affinity between phosphorylated HnoC and the *hnoXp* control region decreases fivefold compared with the unphosphorylated state (Table 1). In contrast, the dissociation constant between phosphorylated HnoC and the *hnoC/Dp* control region remains similar to the unphosphorylated state. Thus, phosphorylation only plays a small role in controlling the affinity of HnoC to its target DNA but instead induces changes in conformation or multimerization.

To determine whether the mobility difference of the phosphorylated HnoC–DNA complexes could be caused by changes in multimerization, we further investigated the oligomerization state of HnoC by size-exclusion chromatography (SEC). Purified HnoC in the unphosphorylated form eluted as a single homogeneous peak with an apparent size of 175 kDa (Fig. 6*C*, dashed line). Next, HnoK and ATP were added to generate phosphorylated HnoC. This sample eluted in two separate peaks in a 1:2 ratio, the smaller peak with an apparent size of 175 kDa and the larger peak with an apparent size of 45 kDa (dashed-dotted line). Addition of inactive H72A HnoK histidine kinase did not lead to formation of the 45-kDa peak (dotted line). The broad peak eluting between 4.3 and 5.5 min corresponds to soluble aggregate of HnoK that forms at the concentration required for efficient HnoC phosphorylation (solid line). Given a mass of 66.3 kDa for the monomeric maltose binding protein (MBP)–HnoC fusion, the smaller species with an apparent size of 45 kDa likely corresponds to an HnoC monomer, whereas the 175-kDa species probably constitutes a tetramer. Consequently, unphosphorylated HnoC was present uniformly as a tightly associated oligomer, whereas phosphorylation of HnoC caused dissociation into monomers. The presence of a small 175-kDa peak in the HnoC, HnoK, and ATP sample suggests that HnoC becomes partially dephosphorylated and reforms a tetramer during the chromatography run.

To confirm that phosphorylation of HnoC causes a change in subunit multimerization in the DNA-bound complex, the stoichiometry between HnoC and the DNA was determined (Fig. 6*D*). The HnoC:control DNA complex was isolated by affinity purification on streptavidin resin using a desthiobiotin tag on the DNA probe. In the unphosphorylated complex, four subunits of HnoC were present per DNA molecule, providing further evidence that HnoC binds to the promoter region as a tetramer. When excess HnoK and ATP were added to phosphorylate HnoC, the stoichiometry of the DNA-bound complex decreased to less than two HnoC subunits per DNA molecule (Fig. 6*D*). The decreased ratio corresponds to the mixture of bound states observed in the gel-shift experiment (Fig. 6 *A* and *B*), confirming that these states represent lower-order HnoC multimers caused by phosphorylation-induced dissociation.

Overall, the SEC experiments and stoichiometry determination complement the results from the gel-shift assay and demonstrate that unphosphorylated HnoC exists as an oligomer. HnoC binds to the control region DNA cooperatively and forms the tightly associated and highly retained band in the gel (Fig. 6 *A* and *B*, *Left*). Phosphorylation by the kinase HnoK and ATP leads to dissociation of the oligomer. Because of incomplete phosphorylation, HnoC monomers are accompanied by a mixture of lower-order oligomers (trimers and dimers) and undissociated tetramers. The lower-order oligomers can still associate to the control region DNA and are likely responsible for the bands at lower retention in the gel-shift assay (Fig. 6 *A* and *B*, *Right*). In contrast to most other DNA-binding response regulators, which form tighter oligomers in the phosphorylated state (11), phosphorylation of HnoC weakens the oligomeric state and promotes subunit dissociation. Therefore, the unphosphorylated form of HnoC represents the repressive state, whereas phosphorylation derepresses transcription.

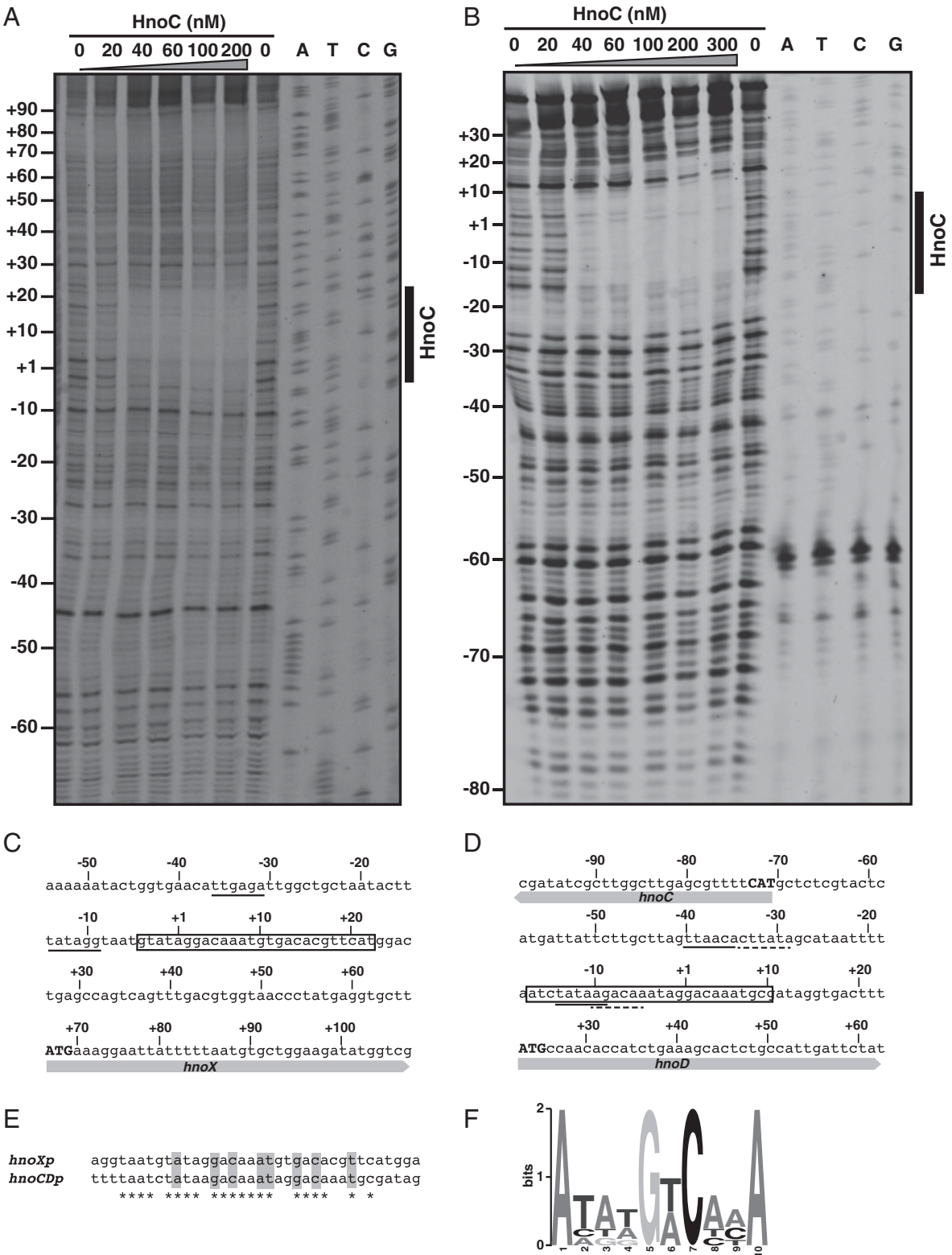


**Fig. 5.** DNase I footprinting of *hno* promoter control regions to map the HnoC binding sites. (*A* and *B*) Gel electrophoresis of DNA fragments of the *hnoX* (*A*) and *hnoC/D* (*B*) promoter control regions from the footprinting analysis. Probes were incubated with increasing amounts of HnoC and digested with DNase I. Protected regions by HnoC are indicated by the black bar on the right. The numbering is relative to the predicted transcription start site of the *hnoX* or *hnoD* gene. (*C* and *D*) Sequence of the hnoX (*C*) and hnoC/D (*D*) promoter region. The predicted −10 and −35 promoter regions are underlined (dashed lines correspond to the *hnoC* promoter elements). The DNA regions protected by HnoC in the footprinting analysis are boxed. (*E*) Alignment of the DNA regions protected by HnoC. Residues forming an inverted repeat are highlighted in gray. (*F*) Consensus sequence for the binding half-site of an HnoC monomer. The motif was generated in MEME (60) from the known binding site in the *hnoX* and *hnoC/D* promoter, and a predicted binding site in the SO2547 promoter region.

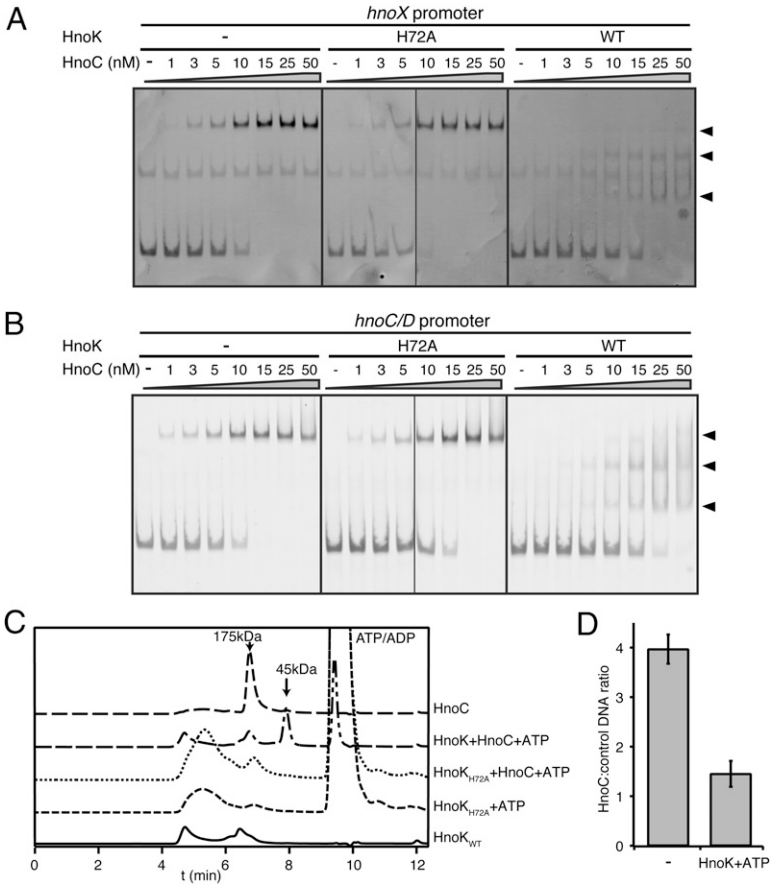


**Fig. 6.** Effect of phosphorylation on HnoC control region binding. (*A* and *B*) Gel-shift binding assay between phosphorylated HnoC and DNA probes (5 nM) of the *hnoX* (*A*) or the *hnoC/D* promoter control region (*B*). HnoC was phosphorylated with excess HnoK and ATP before incubation with the labeled promoter probe or incubated with the inactive H72A HnoK mutant. (*C*) SEC of HnoK, unphosphorylated HnoC, or phosphorylated HnoC incubated with HnoK and ATP. Approximate sizes of HnoC species are indicated and were measured by comparing retention times to molecular weight standards. (*D*) HnoC stoichiometry in the DNA-bound complex. The HnoC:*hnoXp* DNA complex was formed with excess HnoC and affinity-purified using a desthiobiotin tag on the DNA probe. The stoichiometry was calculated as the ratio of HnoC and to DNA concentration. Measurements from nine (without HnoK) or three (+HnoK +ATP) independent experiments were averaged, and the SE is represented by error bars.

## Discussion

Structural and biochemical studies on a large number of DNA-binding response regulators have provided insight into the effects of receiver domain phosphorylation on transcriptional regulation by the DNA-binding domain. Despite some commonalities within subfamilies, the divergence of regulatory mechanisms even between close structural homologs is remarkable (11, 28). HnoC belongs to a relatively small subfamily of DNA-binding response regulators, which thus far has been uncharacterized. The present study on HnoC reveals several surprising and unprecedented regulatory features that expand the repertoire of mechanistic possibilities for DNA-binding response regulators.

SEC and the observation of high cooperativity for HnoC binding to control region DNA demonstrated that unphosphorylated HnoC exists as a tetramer. Response regulator oligomerization is a common regulation method, because most DNA-binding proteins require homodimerization to bind effectively to DNA repeats, which almost always constitute the target sequences. Dimerization has been observed in many response regulator subfamilies, such as for OmpR/PhoB (29–31) and NarL/FixJ members (32, 33). In contrast, it is unlikely that unphosphorylated HnoC exists as a dimer. Instead, the stoichiometry of HnoC:DNA complex, the binding cooperativity with a Hill coefficient of ~3, and the apparent weight of the oligomer, which is much larger than twice the monomeric weight, points to an assembly of HnoC into tetramers (Fig. 6). Nonetheless, the footprinting results only demonstrate protection of a region large enough to accommodate an HnoC dimer. This suggests that two HnoC subunits in the tetramer are not in contact with DNA. A tetrameric HnoC architecture could facilitate binding to two more distantly spaced tandem recognition sequences, for example as observed for OmpR (34). If two tandem repeats are spaced apart, the large DNA–protein complex could have a role in deforming the DNA as suggested from tetrameric complexes of TorR and DosR (35–37). The HnoC tetramer could bind to two separate *hno* promoters simultaneously to bring them into close proximity.

Apart from observed NtrC hexamers, which assemble owing to AAA+ ATPase domains, higher-order oligomerization states are not common. TorR has been suggested to form tetramers based on biochemical evidence (35, 36), and tetramers of the DNA-binding domain of DosR have been observed crystallographically (37), although it is not clear whether these play a role in full-length DosR (38). The OmpR/PhoB-like regulator ArcA has been shown to form oligomers that are possibly larger than tetramers when phosphorylated; however, structural and functional details remain unclear (39, 40). Other response regulators, such as OmpR and PhoB, form higher-order oligomers when dimers or monomers assemble cooperatively on multiple DNA binding sites (24, 34).

The HnoC tetramers form in the unphosphorylated state and bind tightly to the control region around the *hno* promoters. According to the in vivo expression data, this state represses transcription. The footprinting data suggest a model in which the HnoC tetramer occludes RNA polymerase from initiating transcription through steric hindrance (Fig. 7*A*). SEC and the stoichiometry determination of the HnoC:DNA complex demonstrated that HnoC phosphorylation weakens the multimeric interactions, causing dissociation into monomers (Fig. 6 *C* and *D*). Accordingly, the gel-shift assays indicated that multimers of intermediate size could form, which were potentially stabilized by incomplete phosphorylation of the HnoC subunits or by DNA interactions (Fig. 6 *A* and *B*). These lower-order HnoC oligomers can still associate to the control region DNA.

This leads to an overall model in which phosphorylation of HnoC by a cognate kinase, HnoK or HnoS, weakens subunit

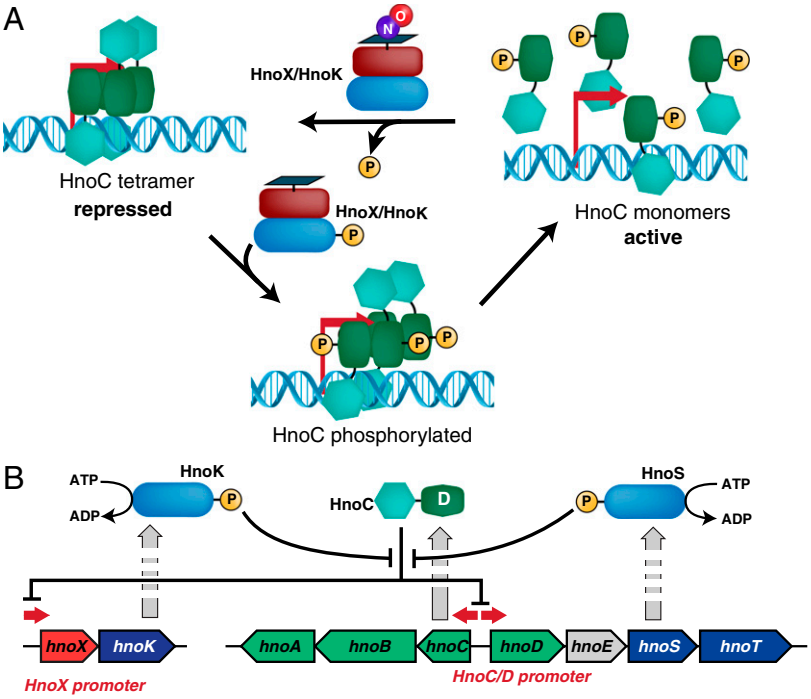


**Fig. 7.** Model for regulation of HnoC in the context of the H-NOX/NO signaling network. (*A*) Model for regulation of HnoC by phosphorylation. Unphosphorylated HnoC forms a tetramer with tight affinity to control regions, which prevents transcription. When phosphorylated by HnoK or HnoS, HnoC tetramers become destabilized and the complex dissociates. The HnoC monomers dissociate from the control region DNA and allow transcription. (*B*) Model for the transcriptional feedback loop in the H-NOX/NO signaling network. HnoC represses transcription from the *hnoX*, *hnoC*, and *hnoD* promoter, inhibiting its own expression and expression of the HnoK kinase. HnoK phosphorylates HnoC and relieves the repression.

interactions, initiating the dissociation of the transcription factor from the control region, and subsequently, the promoter becomes accessible for transcription (Fig. 7*A*). This derepression mechanism through phosphorylation-induced dissociation is unprecedented. It represents a stark contrast to activation of most other response regulator transcription factors, which typically dimerize after phosphorylation and activate transcription through tighter affinity to regulatory sequences near the promoter and subsequent recruitment of RNA polymerase. For instance, members from the OmpR/PhoB family exist as monomers in the unphosphorylated state, and phosphorylation induces dimerization and activation (29–31). Likewise, phosphorylation induces dimerization in NarL (32), which can both positively and negatively regulate gene expression (41). This study demonstrates that phosphorylation of the receiver domain is not limited to promoting subunit dimerization but can also trigger dissociation of response regulator oligomers.

HnoC has been classified as a MerR-like response regulator, on the basis of sequence similarity of the HTH DNA-binding domain to the MerR family (13). MerR family members share an extended α-helix adjacent to the HTH domain as a link to the C-terminal domain. Two helices from separate subunits form an antiparallel coiled-coil involved in dimerization (14, 27). In contrast, the linker region between the DNA-binding domain and receiver domain of HnoC is significantly shorter than the coiled-coil, suggesting a divergent tertiary structure. Alternative subunit interfaces between the response regulator receiver domains, as observed in the receiver domain crystal structure of an HnoC ortholog, could be responsible for tetramer formation (42). Analogous to other MerR proteins, HnoC binds to a dyad of inverted repeats in the promoter, but in the case of HnoC the repeats are not located between the −10 and −35 regions. Likewise, the HnoC-controlled promoters do not show the extended 19- to 20-bp spacing between the −10 and −35 regions, which is a characteristic of MerR promoters. Therefore, HnoC exerts transcriptional control through a different mechanism than MerR. The latter activates transcription through partial unwinding of the promoter DNA and alignment of the −10 and −35 site for proper RNAP interaction (14, 25, 27). Instead, HnoC binding blocks the −35 or −10 region and the transcription start site and thus represses gene expression. Because of its divergent structural properties and mechanism of transcriptional control, the HnoC response regulator should be considered separate from the MerR family.

HnoC acts as a transcriptional regulator in the larger context of the H-NOX/NO (*hno*) signaling network, which senses NO and stimulates a change in bacterial motility by inducing surface adhesion in biofilms (6). Along with HnoB and HnoD, HnoC is one of three phosphotransfer targets of the histidine kinases HnoK and HnoS (Fig. 1*A*) (6). This study demonstrates that HnoC is a transcriptional regulator for all of the signaling components in the pathway, repressing transcription from each of the three *hno* promoters. Because HnoC represses expression of itself and the kinases, an autoregulatory feedback loop is created (Fig. 7*B*).

Feedback control is a common feature in prokaryotic and eukaryotic signal transduction systems (43) and serves a multitude of functions (44–47). In bacteria, autoregulation of transcription factors through a negative feedback loop occurs especially frequently (46, 48), whereas positive feedback loops are more prevalent in two-component signaling systems (49). Overall, feedback control allows for fine-tuning of the temporal dynamics of the signaling system. For instance, positive feedback loops create an initial activation surge in transcription, slow down the response time to a stimulus, broaden the cell-to-cell variability, or can be associated with learning behavior (44, 47, 50, 51). In contrast, negative feedback loops speed up the response time to a stimulus, produce a more uniform output level, achieve adaptation, or produce oscillation under certain conditions (45–47, 52, 53).

Transcriptional feedback in the *hno* signaling system is complicated because repression is influenced by HnoC phosphorylation and the level of phosphorylated HnoC is governed by the activity of two kinases, each possessing a different input signal. Furthermore, expression of HnoK and HnoS kinase, as well as the HnoX NO sensor, is itself autoregulated through the feedback loop (Fig. 7*B*). In the absence of NO, HnoK is active as a kinase (10), causing phosphotransfer to HnoC and consequently high expression of the *hno* signaling genes. When NO concentrations rise, HnoK can act as a phosphatase (6), consequently

dephosphorylating HnoC, which represses expression of the *hno* signaling genes. In the reporter assays in *S. oneidensis*, only a modest increase in GFP expression was observed when *hnoX* was deleted, whereas the *hnoK* deletion did not cause a significant change in steady-state GFP levels (Fig. 3*A*). This is not surprising, given the complex connectivities of the network, which integrates the kinase and phosphatase activity of HnoK and HnoS, as well as the expression levels of each protein. Dynamic changes in expression of signaling components will likely be more pronounced but at the same time more challenging to detect. Because expression of all signaling genes in the network, including HnoB and HnoD, is influenced by the feedback loop, phosphodiesterase activity and cyclic-di-GMP levels are equally affected. For instance, shifts to high NO concentrations will not only inactivate HnoB and HnoD but will also lower the expression levels of both proteins. This would accelerate the buildup of cyclic-di-GMP concentrations and biofilm formation. In contrast, a shift to lower NO levels could produce a temporary surge in HnoB expression, along with all other signaling proteins. Taking into account the increased phosphotransfer by HnoK, this would intensify the phosphodiesterase activity and accelerate the clearance of cyclic-di-GMP. Consequently, the transcriptional feedback loop has an important role in regulating the NO response dynamics in the entire network.

## Materials and Methods

**Strain and Plasmid Generation, Media, and Growth Conditions.** Detailed protocols can be found in *SI Materials and Methods*. Strains, plasmids, and primers used in this study are listed in Tables S1 and S2.

**Microarray Analysis.** Four biological replicates of WT *S. oneidensis* MR-1 and Δ*hnoC* were grown in 12-well microtiter plates inside an anaerobic glovebag (Coy Laboratory Products). After 15 h, 2.5 mL of the culture were treated with RNAprotect (Qiagen), and total RNA was extracted from the samples using the RNeasy mini kit (Qiagen). The quality of the RNA was assessed on a Bioanalyzer. Cy5-labeled cRNA was generated using the Low Input Quick Amp WT Labeling Kit (Agilent) with 100 ng of input RNA. A custom whole-genome microarray for *S. oneidensis* MR-1, containing a minimum of three probes for each gene, was designed on eArray (Agilent). The samples were hybridized onto individual arrays using standard protocols provided by Agilent. The microarray data were analyzed using the *limma* package in the *R* computing environment (54–56). Data were background corrected using the normexp method with an offset of 1 and quantile normalized between arrays. Replicate probes were averaged, the data were fit to a linear model, and differentially expressed genes between strains were filtered using an adjusted *P* value smaller than 0.05 and a fold-change between samples of at least 2. The microarray data have been deposited in the National Center for Biotechnology Information's GEO database (57) and can be accessed under reference number GSE44689.

**GFP-Reporter Assays.** *S. oneidensis* strains, transformed with the appropriate reporter plasmids, were grown aerobically in LB until exponential phase ($OD_{600}$ ~0.5). Fifteen to twenty microliters of each culture were diluted into 2 mL of prechilled 1.5× PBS solution. Samples were analyzed on a BD LSR II flow cytometer using a forward-scatter and side-scatter threshold of 300 V. The laser settings were as follows: Forward scatter (FSC): 580 V; Side scatter (SSC): 328 V; FITC: 610 V. Each dataset, consisting of 30,000 observations, was gated manually by FSC area and SSC area and subsequently by SSC area and SSC width to exclude doublets. GFP expression was calculated as the median FITC intensity. The fluorescence intensities from three biological replicates, grown on separate days, were normalized to the intensity of *S. oneidensis* Tn7::*gfp*, a strain expressing GFP constitutively from a transposon insertion.

**HnoC and HnoK Expression and Purification.** To ensure solubility, HnoC and HnoK were expressed and purified as a C-terminal fusion to MBP. The expression and purification was performed as previously described (6).

**DNA Gel-Shift Assays.** DNA probes (250-300 bp) of the *hnoX*, *hnoC/D*, and *ompR* promoter control regions were generated by PCR amplication from *S. oneidensis* genomic DNA using the respective hno_-F and hno_-R primers. The forward primer contained a 5′-6-carboxyfluorescein modification to incorporate a fluorescence label into each probe. Identical unmodified forward primers were used to create unlabeled DNA probes for the competition assay. Gel-shift assays were performed as previously described (58) with the following modifications: Each binding reaction (20 μL) contained 5 nM DNA probe, 1–500 nM HnoC, 300 μg $mL^{-1}$ BSA, 50 μg $mL^{-1}$ Poly(dI-dC)·Poly(dI-dC), and 10% (vol/vol) glycerol in binding buffer [50 mM Tris (pH 8.0), 50 mM NaCl, 5 mM $MgCl_2$, and 2 mM DTT]. If needed, a 25-fold excess unlabeled competitor probe (125 nM) was added. To examine the effect of phosphorylating HnoC on DNA-binding, 5 μM HnoK and 1 mM ATP were added to the respective binding reactions. Each reaction was incubated for 30 min at room temperature and loaded without loading dye onto precast 6% DNA Retardation Gels (Life Technologies). The samples were separated by gel electrophoresis in 0.5× TBE running buffer (44.5 mM Tris, 44.5 mM boric acid, and 1 mM EDTA) at 100 V for 1.5 h. The gels were imaged on a Pharos FX System (Bio-Rad) using a laser excitation at 488 nm and a band-pass 530 nm filter. Band intensities were quantified using Image Lab software (Bio-Rad).

**SEC and Determination of HnoC:Control DNA Stoichiometry.** SEC was performed on a Bio SEC-3, 300-Å, 4.6 × 300-mm column (Agilent) in 50 mM sodium phosphate (pH 8.0), 150 mM NaCl at 10 °C at a flow rate of 0.4 mL $min^{-1}$. Samples of HnoC (10 μM), or HnoC phosphorylated with fivefold excess HnoK and ATP as before, were filtered and 10-μL portions injected. For determination of the HnoC stoichiometry in the DNA bound complex, the *hnoXp* control DNA probe was PCR amplified using a reverse primer containing a 5′-desthiobiotin modification for affinity purification of the DNA:protein complex. The complex was formed as described for the gel-shift assays using 200–400 nM HnoC and 5–10 nM *hnoXp* probe. Subsequently, streptavidin beads (50 μL) were added and incubated with the complex for 30 min under gentle agitation. The supernatant was removed, and the beads were washed two times with 500 μL binding buffer until unbound HnoC was no longer detectable in the wash. The HnoC:DNA complex was eluted with 100 μL biotin (20 mM) in binding buffer. Native gel electrophoresis confirmed that the complex was intact and that no unbound DNA was present. The amount of DNA in the complex was quantified from the fluorescence signal of the DNA probe in the gel. A standard curve was generated from DNA samples of known concentrations in the same gel. The HnoC concentration was quantified by Western blot using a primary antibody against the $His_6$-tag of HnoC and a standard curve of known HnoC concentrations in the same Western blot. The HnoC:DNA stoichiometry was calculated as the ratio of HnoC to DNA concentration.

**DNase I Footprinting.** The same DNA probe from the gel-shift assay, containing a 5′-6-carboxyfluorescein modification, was used for the *hnoXp* control region. For the *hnoCD* control region, a shorter 137-bp fragment was PCR amplified, also using one primer containing a 5′-6-carboxyfluorescein modification. The footprinting protocol was modified from the literature (59). The binding reactions (100 μL) consisted of 40 nM DNA probe, 0–300 nM HnoC, 300 μg $mL^{-1}$ BSA, 5 μg $mL^{-1}$ Poly(dI-dC)·Poly(dI-dC), 50 mM Tris (pH 8.0), 50 mM NaCl, 5 mM $MgCl_2$, 2 mM DTT, and 10% (vol/vol) glycerol. After incubation at 25 °C for 30 min, 60 ng DNase I was added. After 1 min, the reactions were quenched by addition of 100 μL 192 mM sodium acetate, 32 mM EDTA, 0.14% SDS, and 64 μg/mL yeast RNA. The samples were phenol/chloroform extracted, and the DNA was precipitated in ethanol. DNA fragments were resuspended in 10 μL Tris/EDTA buffer and 10 μL 95% (vol/vol) formamide, 25 mM EDTA, boiled for 5 min, and separated on a 6% polyacrylamide, 7.5 M urea sequencing gel. The gels were imaged on a Pharos FX System (Bio-Rad) using a laser excitation at 488 nm and a band-pass 530 nm filter. A Sanger sequencing ladder was generated using the Thermo Sequencing Dye Primer Manual Cycle Sequencing Kit (Affymetrix) and the same fluorescently labeled primer for generating the DNA probes.

**ACKNOWLEDGMENTS.** We thank Prof. Alfred Spormann (Stanford University) and Ian Marshall for *S. oneidensis* strains, the microarray design, and help with protocols; Justin Choi at the Berkeley Functional Genomics Lab for assistance with the microarray analysis; members of the M.A.M. laboratory for helpful discussions and critical reading of the manuscript; and the Joyce laboratory (The Scripps Research Institute) for use of their Pharox FX gel imager and assistance with the DNA sequencing gels. The work was supported by National Institutes of Health Grant GM 070671. This is TSRI manuscript #23015.

1. Donlan RM, Costerton JW (2002) Biofilms: Survival mechanisms of clinically relevant microorganisms. *Clin Microbiol Rev* 15(2):167–193.

2. Costerton JW, Stewart PS, Greenberg EP (1999) Bacterial biofilms: A common cause of persistent infections. *Science* 284(5418):1318–1322.

3. Römling U, Balsalobre C (2012) Biofilm infections, their resilience to therapy and innovative treatment strategies. *J Intern Med* 272(6):541–561.
4. Stanley NR, Lazazzera BA (2004) Environmental signals and regulatory pathways that influence biofilm formation. *Mol Microbiol* 52(4):917–924.
5. MacMicking J, Xie QW, Nathan C (1997) Nitric oxide and macrophage function. *Annu Rev Immunol* 15:323–350.
6. Plate L, Marletta MA (2012) Nitric oxide modulates bacterial biofilm formation through a multicomponent cyclic-di-GMP signaling network. *Mol Cell* 46(4):449–460.
7. Barraud N, et al. (2009) Nitric oxide signaling in *Pseudomonas aeruginosa* biofilms mediates phosphodiesterase activity, decreased cyclic di-GMP levels, and enhanced dispersal. *J Bacteriol* 191(23):7333–7342.
8. Carlson HK, Vance RE, Marletta MA (2010) H-NOX regulation of c-di-GMP metabolism and biofilm formation in *Legionella pneumophila*. *Mol Microbiol* 77(4):930–942.
9. Liu N, et al. (2012) Nitric oxide regulation of cyclic di-GMP synthesis and hydrolysis in *Shewanella woodyi*. *Biochemistry* 51(10):2087–2099.
10. Price MS, Chao LY, Marletta MA (2007) *Shewanella oneidensis* MR-1 H-NOX regulation of a histidine kinase by nitric oxide. *Biochemistry* 46(48):13677–13683.
11. Gao R, Stock AM (2010) Molecular strategies for phosphorylation-mediated regulation of response regulator activity. *Curr Opin Microbiol* 13(2):160–167.
12. Stock AM, Robinson VL, Goudreau PN (2000) Two-component signal transduction. *Annu Rev Biochem* 69:183–215.
13. Galperin MY (2010) Diversity of structure and function of response regulator output domains. *Curr Opin Microbiol* 13(2):150–159.
14. Brown NL, Stoyanov JV, Kidd SP, Hobman JL (2003) The MerR family of transcriptional regulators. *FEMS Microbiol Rev* 27(2-3):145–163.
15. Miller WG, Leveau JH, Lindow SE (2000) Improved gfp and inaZ broad-host-range promoter-probe vectors. *Mol Plant Microbe Interact* 13(11):1243–1250.
16. Andersen JB, et al. (1998) New unstable variants of green fluorescent protein for studies of transient gene expression in bacteria. *Appl Environ Microbiol* 64(6): 2240–2246.
17. Davies KM, Lowe ED, Vénien-Bryan C, Johnson LN (2009) The HupR receiver domain crystal structure in its nonphospho and inhibitory phospho states. *J Mol Biol* 385(1): 51–64.
18. Lauriano CM, Ghosh C, Correa NE, Klose KE (2004) The sodium-driven flagellar motor controls exopolysaccharide expression in *Vibrio cholerae*. *J Bacteriol* 186(15): 4864–4874.
19. Kenney LJ (2002) Structure/function relationships in OmpR and other winged-helix transcription factors. *Curr Opin Microbiol* 5(2):135–141.
20. Blanco AG, Canals A, Bernués J, Solà M, Coll M (2011) The structure of a transcription activation subcomplex reveals how σ(70) is recruited to PhoB promoters. *EMBO J* 30(18):3776–3785.
21. Su W, Porter S, Kustu S, Echols H (1990) DNA-looping and enhancer activity: Association between DNA-bound NtrC activator and RNA polymerase at the bacterial glnA promoter. *Proc Natl Acad Sci USA* 87(14):5504–5508.
22. Gusa AA, Scott JR (2005) The CovR response regulator of group A streptococcus (GAS) acts directly to repress its own promoter. *Mol Microbiol* 56(5):1195–1207.
23. Harlocker SL, Bergstrom L, Inouye M (1995) Tandem binding of six OmpR proteins to the ompF upstream regulatory sequence of *Escherichia coli*. *J Biol Chem* 270(45): 26849–26856.
24. Blanco AG, Sola M, Gomis-Rüth FX, Coll M (2002) Tandem DNA recognition by PhoB, a two-component signal transduction transcriptional activator. *Structure* 10(5): 701–713.
25. O'Halloran TV, Frantz B, Shin MK, Ralston DM, Wright JG (1989) The MerR heavy metal receptor mediates positive activation in a topologically novel transcription complex. *Cell* 56(1):119–129.
26. Li J, Kustu S, Stewart V (1994) In vitro interaction of nitrate-responsive regulatory protein NarL with DNA target sequences in the fdnG, narG, narK and frdA operon control regions of *Escherichia coli* K-12. *J Mol Biol* 241(2):150–165.
27. Heldwein EE, Brennan RG (2001) Crystal structure of the transcription activator BmrR bound to DNA and a drug. *Nature* 409(6818):378–382.
28. Batchelor JD, et al. (2008) Structure and regulatory mechanism of *Aquifex aeolicus* NtrC4: Variability and evolution in bacterial transcriptional regulation. *J Mol Biol* 384(5):1058–1075.
29. Gao R, Tao Y, Stock AM (2008) System-level mapping of *Escherichia coli* response regulator dimerization with FRET hybrids. *Mol Microbiol* 69(6):1358–1372.
30. Bachhawat P, Swapna GVT, Montelione GT, Stock AM (2005) Mechanism of activation for transcription factor PhoB suggested by different modes of dimerization in the inactive and active states. *Structure* 13(9):1353–1363.
31. McCleary WR (1996) The activation of PhoB by acetylphosphate. *Mol Microbiol* 20(6): 1155–1163.
32. Maris AE, et al. (2002) Dimerization allows DNA target site recognition by the NarL response regulator. *Nat Struct Biol* 9(10):771–778.
33. Da Re S, et al. (1999) Phosphorylation-induced dimerization of the FixJ receiver domain. *Mol Microbiol* 34(3):504–511.
34. Huang KJ, Lan CY, Igo MM (1997) Phosphorylation stimulates the cooperative DNA-binding properties of the transcription factor OmpR. *Proc Natl Acad Sci USA* 94(7): 2828–2832.
35. Simon G, et al. (1995) Binding of the TorR regulator to cis-acting direct repeats activates tor operon expression. *Mol Microbiol* 17(5):971–980.
36. Ansaldi M, Simon G, Lepelletier M, Méjean V (2000) The TorR high-affinity binding site plays a key role in both torR autoregulation and torCAD operon expression in *Escherichia coli*. *J Bacteriol* 182(4):961–966.
37. Wisedchaisri G, et al. (2005) Structures of *Mycobacterium tuberculosis* DosR and DosR-DNA complex involved in gene activation during adaptation to hypoxic latency. *J Mol Biol* 354(3):630–641.
38. Wisedchaisri G, Wu M, Sherman DR, Hol WGJ (2008) Crystal structures of the response regulator DosR from *Mycobacterium tuberculosis* suggest a helix rearrangement mechanism for phosphorylation activation. *J Mol Biol* 378(1):227–242.
39. Toro-Roman A, Mack TR, Stock AM (2005) Structural analysis and solution studies of the activated regulatory domain of the response regulator ArcA: A symmetric dimer mediated by the alpha4-beta5-alpha5 face. *J Mol Biol* 349(1):11–26.
40. Jeon Y, Lee YS, Han JS, Kim JB, Hwang DS (2001) Multimerization of phosphorylated and non-phosphorylated ArcA is necessary for the response regulator function of the Arc two-component signal transduction system. *J Biol Chem* 276(44):40873–40879.
41. Darwin AJ, Tyson KL, Busby SJ, Stewart V (1997) Differential regulation by the homologous response regulators NarL and NarP of *Escherichia coli* K-12 depends on DNA binding site arrangement. *Mol Microbiol* 25(3):583–595.
42. Patskovsky Y, et al. (2011) Crystal structure of response regulator (signal receiver domain) from *Bermanella marisrubri*. 10.2210/pdb3lte/pdb.
43. Brandman O, Meyer T (2008) Feedback loops shape cellular signals in space and time. *Science* 322(5900):390–395.
44. Mitrophanov AY, Groisman EA (2008) Positive feedback in cellular control systems. *Bioessays* 30(6):542–555.
45. Ma W, Trusina A, El-Samad H, Lim WA, Tang C (2009) Defining network topologies that can achieve biochemical adaptation. *Cell* 138(4):760–773.
46. Rosenfeld N, Elowitz MB, Alon U (2002) Negative autoregulation speeds the response times of transcription networks. *J Mol Biol* 323(5):785–793.
47. Alon U (2007) Network motifs: Theory and experimental approaches. *Nat Rev Genet* 8(6):450–461.
48. Thieffry D, Huerta AM, Pérez-Rueda E, Collado-Vides J (1998) From specific gene regulation to genomic networks: A global analysis of transcriptional regulation in *Escherichia coli*. *Bioessays* 20(5):433–440.
49. Goulian M (2010) Two-component signaling circuit structure and properties. *Curr Opin Microbiol* 13(2):184–189.
50. Shin D, Lee EJ, Huang H, Groisman EA (2006) A positive feedback loop promotes transcription surge that jump-starts *Salmonella* virulence circuit. *Science* 314(5805): 1607–1609.
51. Hoffer SM, Westerhoff HV, Hellingwerf KJ, Postma PW, Tommassen J (2001) Autoamplification of a two-component regulatory system results in "learning" behavior. *J Bacteriol* 183(16):4914–4917.
52. Becskei A, Serrano L (2000) Engineering stability in gene networks by autoregulation. *Nature* 405(6786):590–593.
53. Mitrophanov AY, Churchward G, Borodovsky M (2007) Control of *Streptococcus pyogenes* virulence: Modeling of the CovR/S signal transduction system. *J Theor Biol* 246(1):113–128.
54. Smyth GK (2004) Linear models and empirical bayes methods for assessing differential expression in microarray experiments. *Stat Appl Genet Mol Biol* 3:Article3.
55. Smyth GK, Speed T (2003) Normalization of cDNA microarray data. *Methods* 31(4): 265–273.
56. Ritchie ME, et al. (2007) A comparison of background correction methods for two-colour microarrays. *Bioinformatics* 23(20):2700–2707.
57. Edgar R, Domrachev M, Lash AE (2002) Gene Expression Omnibus: NCBI gene expression and hybridization array data repository. *Nucleic Acids Res* 30(1):207–210.
58. Buratowski S, Chodosh LA (2001) Mobility shift DNA-binding assay using gel electrophoresis. *Curr Protoc Pharmacol* Chapter 6:Unit 6.8–Unit 8.
59. Bordi C, et al. (2004) Genes regulated by TorR, the trimethylamine oxide response regulator of *Shewanella oneidensis*. *J Bacteriol* 186(14):4502–4509.
60. Bailey TL, Elkan C (1994) Fitting a mixture model by expectation maximization to discover motifs in biopolymers. *Proc Int Conf Intell Syst Mol Biol* 2:28–36.